Effects of acid anions, major metallic elements, and chlorides on Li detection by DFWM in graphite furnace

Kun Fei (费 坤), Xuemei Cheng (程雪梅)*, Xunli Yin (尹逊莉), Haowei Chen (陈浩伟), Jintao Bai (白晋涛), and Zhaoyu Ren (任兆玉)**

State Key Lab Incubation Base of Photoelectric Technology and Functional Materials, National Photoelectric Technology, and Functional Materials and Application of Science and Technology International Cooperation Center, Northwest University, Xi'an 710069, China

**Corresponding author: chengxuemei111@sina.com.cn; **corresponding author: rzy@nwu.edu.cn*

Received August 9, 2014; accepted October 24, 2014; posted online December 3, 2014

In trace Li analysis with degenerate four-wave mixing (DFWM) method, acid anions and major metallic elements are dominant interferences in Li-containing samples. To better use DFWM technique to analyze trace Li in actual samples, we study their effects on Li DFWM signal intensity. It is found that K, Cs, and Ni can enhance the Li DFWM signal, SO_4^{2-}, PO_4^{3-}, Cl^-, and Ca can cause significant suppression, and NO_3^-, Mg, Ba, Sr, and Na almost have no effects. Finally, we use H_3BO_3 to eliminate the depressive effects of chlorides on Li DFWM signal. The result is also of reference in other trace elements analysis with DFWM.

OCIS codes: 300.2570, 300.6290, 190.4380.
doi: 10.3788/COL201412.123001.

Trace Li analysis is of fundamental importance in geology[1], environmentology, physical science[2], and human health[3]. It can be analyzed by multiple techniques such as inductively coupled plasma mass spectrometry (ICP-MS), neutron activation analysis (NAA)[4], flame emission (FE)[5], and atomic absorption spectrometry (AAS)[3]. ICP-MS and NAA can provide good sensitivity. However, the complex sample pre-treatment[6] and the exorbitant price limit the wide application of NAA and ICP-MS in trace analysis of element. FE is a simple and cheap technique. However, it has a poor signal-to-noise ratio. AAS as a basic linear optical spectrometry has shown high resolution and low detection limit, which is widely used in trace element detection.

Compared with linear optical spectrometry, nonlinear spectroscopic techniques are getting more and more attention for its outstanding advantages in spectral resolution and detection sensitivity[7]. Especially, the degenerate four-wave mixing (DFWM) based on the third-order nonlinear interaction of light and matter is of particular interest in trace analysis. As a kind of sub-Doppler method, DFWM has very high spectral resolution, good species, and quantum state selectivity. Moreover, DFWM has very good sensitivity and can reflect the subtle sample concentration variation for its intensity is in proportional to the square of the sample concentration[8]. Besides, DFWM has special advantages in gaseous samples analysis because it is the most efficient nonlinear process generating in isotropic medium. Simultaneously, as a multiwave mixing process, it can also be enhanced by the dressing beams[9] or electromagnetically induced transparency[10]. Based on the above merits, DFWM has been successfully applied to detect various transient[11] and stable[12] species in combustion processes, and metallic atomic vapor sample[7,13] since it was firstly used in the detection of OH in a flame by Ewart *et al.*[14] in 1986.

To analyze the metallic elements in solid and liquid samples with DFWM, an atomizer is needed to obtain the gaseous atoms. As a type of atomizer, the graphite furnace is widely used with the advantages of fast heating speed, high sensitivity, and adjustable temperature. More importantly, it just needs a small amount of sample during measurement, which makes a great contribution in non-destructive testing. Previously, our group has employed a graphite furnace to quantitatively measure Rb isotope ratio in RbCl sample using DFWM, and obtained the detection limit as low as 18.41 fg·mL^{-1}[15].

However in practical measurement, there exist multitude physical and chemical reactions between the analyte and matrix constituents in the atomizer, which is known as matrix effect. Matrix effect is an important issue in analytical chemistry, especially in trace element analysis, which may enhance or suppress the detected signal[16,17]. Therefore, to better use DFWM to analyze trace Li in actual samples, it is necessary to investigate the effects of abundant impurities on the DFWM signal of Li. Major metallic elements and acid anions are known to be the dominant interferences[18–22] and widely exist in biological and environmental samples. That is, the concomitant ions in the sample can cause Li forming volatile or stable molecules, which may reduce or increase free Li atoms and further influence DFWM signal intensity. Simultaneously, acids are needed to dissolve the solid samples, the acid anions of which may also influence the Li DFWM

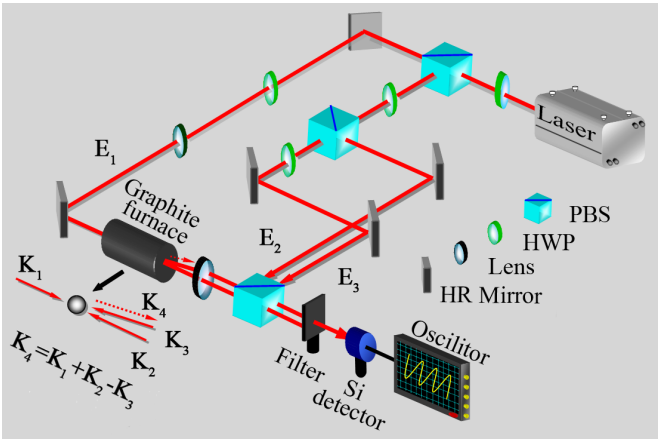

Fig. 1. Scheme of the DFWM experimental setup. The inset is spatial phase-matching geometry used in our work.

signal. Therefore, it is important to make clear of their effects on DFWM signal of Li.

In this letter, we take a graphite furnace as the atomizer and analyze Li element in Li_2CO_3 with the DFWM method. DFWM signal is generated between the transition of $|2S_{1/2}\rangle \rightarrow |2P_{3/2}\rangle$ of ^{7}Li at 670.9385 nm. Acid anions, major metallic elements, and chlorides are mixed into Li_2CO_3 samples as matrices and their effects on DFWM signal intensity of Li are studied respectively. Eventually, based on the research of the effects of chlorides on DFWM signal intensity, H_3BO_3 is taken as a modifier to eliminate the depressive effects of chlorides on Li analysis in NaCl samples.

The induced third-order atomic polarization $P^{(3)}$ is derived from the perturbation theory[15] as

$$P^{(3)} = \frac{N\mu\Omega_1\Omega_2\Omega_3^* e^{i\omega_1 t}}{(\Delta_1 - i\gamma_1)(\Delta_2 - i\gamma_1)(i\gamma_0)}, \quad (1)$$

where $\Delta_i = \omega_i - \omega_o (i = 1, 2)$ is the frequency detuning, $\Omega_i (i = 1, 2, 3)$ is the Rabi frequency, μ is the dipole matrix element, γ_1 is the dipole relaxation rate, γ_0 is the ground state dephasing rate, and N is the atomic number density. DFWM amplitude is obtained by solving the coupling wave equations with the steady-state approximation as

$$E_4(z) = \frac{i\omega^2 P^{(3)} z}{2\xi_0 cn}. \quad (2)$$

Since DFWM signal intensity I is proportional to $|E_4|^2$, I is proportional to the square of the atomic number density N, that is $I \propto N^2$.

The experimental setup and the spatial phase-matching geometry are shown in Fig. 1. A tunable dye-ring-cavity laser (Spectra-Physics, Matisse DR) in CW mode serves as the light source at 670.9385 nm. The laser output is split into three beams $\mathbf{E}_1$, $\mathbf{E}_2$, and $\mathbf{E}_3$ by polarizing beam splitters (PBSs) combined with half-wave plates (HWPs). $\mathbf{E}_1$ and $\mathbf{E}_2$ are the pump fields and $\mathbf{E}_3$ is the probe field. $\mathbf{E}_1$ and $\mathbf{E}_2$ counter-propagate and $\mathbf{E}_3$ is incident at a small angle (less than 0.01 rad) with respect to $\mathbf{E}_2$. The three beams interact with the free Li atoms in the graphite tube together and DFWM signal $\mathbf{E}_4$ is generated simultaneously when phase-matching condition is satisfied. According to the phase-matching condition[23] $\mathbf{k}_1 = -\mathbf{k}_2$, $\mathbf{k}_3 = -\mathbf{k}_4$, DFWM signal $\mathbf{E}_4$ propagates in the opposite direction of $\mathbf{E}_3$. DFWM signal is detected by a silicon detector after $\mathbf{E}_1$ is blocked by a filter. The powers of $\mathbf{E}_1$ and $\mathbf{E}_2$ are set to be 20 mW, and the power of probe beam $\mathbf{E}_3$ is set to be 5 mW.

A graphite furnace (HGS-II, Shenyang Huaguang Precise Instrument Co. Ltd) is used as the atomizer in the experiment. Pyrolytic-coated graphite platforms are used. The optimum temperature program for furnace atomization is given in Table 1.

Different samples experience various atomization processes in the graphite furnace. For $LiNO_3$, Li_2CO_3, Li_2SO_4, and Li_3PO_4 samples, they firstly decompose into Li_2O and then be reduced into free Li atoms by the dense carbon atoms under the higher temperature. The atomization process is presented as[24]

$$LiNO_3, Li_2CO_3, Li_2SO_4, Li_3PO_4\,(l, s) \xrightarrow{\Delta} Li_2O\,(s) \xrightarrow{\Delta} Li_2O\,(l) \xrightarrow{C} Li(g).$$

For metal chlorides, they can be directly dissociated into free metallic atoms and chlorine atoms. The thermal dissociation process is presented as

$$R(Cl)(l, s) \xrightarrow{\Delta} R(Cl)(g) \xrightarrow{\Delta} M(g) + Cl(g).$$

Analyte solutions of different concentrations are prepared fresh by diluting Li_2CO_3 (GB/T602-2002, Tianjin Aoran Fine Chemical Research Institute) solution containing 1 g·L^{-1} Li with distilled water. A 4 g·L^{-1} K solution is prepared by dissolving 10.36 g KNO_3 into 1 L distilled water. Then other K solution with different concentrations are obtained by diluting 4 g·L^{-1} K solution. With the same method, other metallic elements solutions with various concentrations are obtained by diluting the corresponding reagents in the distilled water. Similarly, chlorides containing 10 μg·mL^{-1} Cl^- and acids with different volume fractions can also be obtained.

When the solid samples are measured by DFWM technique, acids are needed for sample dissolution, the acid anions of which may also influence the Li DFWM signal. Therefore, the interference of the commonly used acid anions on DFWM signal intensity should be studied, such as NO_3^-, SO_4^{2-}, PO_4^{3-}, and Cl^-. About 300 ng·mL^{-1} Li solutions are obtained by mixing 600 ng·mL^{-1} Li_2CO_3 solution with HCl, H_3PO_4, H_2SO_4, and HNO_3

Table 1. Time Temperature Program for Li Detection by DFWM

Step	Temperature (°C)	Ramp (s)	Hold (s)	Gas Flow Rate ($mL \cdot min^{-1}$)
Drying	120	10	10	300
Ashing	500	10	15	300
Atomizing	2400	1	5	0
Cleaning	2700	1	3	300

solutions of the same volume at various concentrations. We measured the DFWM signal of Li in pure Li_2CO_3 solution with 300 $ng \cdot mL^{-1}$ Li in it, and then measured the DFWM signals of Li in the abovementioned mixtures. The measured Li DFWM signal intensity data are all normalized to the one obtained with pure Li_2CO_3 solution. The results are collected and plotted in Fig. 2 with respect to the concentrations of the matrix solutions.

It can be seen that HNO_3 has no effect on the DFWM signal intensity. The signal intensity remains constant with HNO_3 concentration increasing. Comparatively, HCl suppresses Li DFWM signal at the largest degree, followed by H_3PO_4 and H_2SO_4. Moreover, the suppression enhances with the concentrations of increasing H_2SO_4, H_3PO_4, and HCl.

When we mix these acids into Li_2CO_3 sample, LiCl, $LiNO_3$, Li_2SO_4, and Li_3PO_4 molecules can be generated. Compared with Li_2CO_3, LiCl, Li_2SO_4, and Li_3PO_4 represent stronger thermal stability. According to the atomization process, LiCl is often hard to dissociate into free Li atoms at the atomization stage, and a part of them even escape out of the graphite furnace at the ashing stage. For Li_2SO_4 and Li_3PO_4, they decompose into the Li_2O incompletely. And therefore, the population of Li free atoms is reduced at the atomization stage according to their atomization processes. That is, Li is partly lost as the forms of LiCl, Li_2SO_4, and Li_2PO_4, and therefore the total number of Li atoms is reduced and Li DFWM signal intensity decreases accordingly. Conversely, $LiNO_3$ molecule has the similar thermal stability with Li_2CO_3. According to the atomization process of $LiNO_3$, it will decompose into Li_2O completely and then be reduced into the free Li atoms. Therefore, the free Li atoms can be kept inside of the graphite furnace and Li DFWM signal intensity is unaffected by NO_3^-.

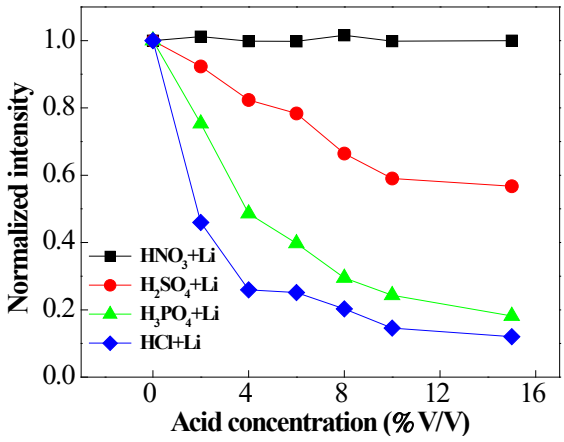

Fig. 2. Normalized Li (300 $ng \cdot mL^{-1}$) DFWM signal intensity containing various acids at different concentrations.

Major metallic elements are known to be the dominant interferences for trace Li analysis and are widely existed in many actual samples, such as salt lakes and minerals. According to the certified values of standard rock samples (GSR3), Ca (58.94 $mg \cdot g^{-1}$), Mg (46.62 $mg \cdot g^{-1}$), Na (25.38 $mg \cdot g^{-1}$), K (19.25 $mg \cdot g^{-1}$), Sr (1100 $\mu g \cdot g^{-1}$), Ba (527 $\mu g \cdot g^{-1}$), Ni (140 $\mu g \cdot g^{-1}$), and Cs (0.7 $\mu g \cdot g^{-1}$) are major metallic elements. Therefore, the effects of these elements on Li DFWM signal should be investigated. Considering NO_3^- almost has no effect on DFWM signal from the investigation above, therefore we take $CsNO_3$, KNO_3, $NaNO_3$, $Mg(NO_3)_2$, $Ni(NO_3)_2$, $Sr(NO_3)_2$, $Ca(NO_3)_2$, and $Ba(NO_3)_2$ as the matrices to study the effects of Cs, K, Mg, Ni, Sr, Ca, Ba, and Na on Li DFWM signal, respectively. About 300 $ng \cdot mL^{-1}$ Li sample solutions are obtained by mixing 600 $ng \cdot mL^{-1}$ Li_2CO_3 solution containing 600 $ng \cdot mL^{-1}$ Li with $Mg(NO_3)_2$, $Ni(NO_3)_2$, $Sr(NO_3)_2$, $Ca(NO_3)_2$, $Ba(NO_3)_2$, KNO_3, $NaNO_3$, and $CsNO_3$ of the same volume at various concentrations. Li DFWM signals are measured with these mixtures in sequence. Similarly, the measured data are all normalized to the obtained pure 300 $ng \cdot mL^{-1}$ Li_2CO_3 solution with 300 $ng \cdot mL^{-1}$ Li. The results are collected and plotted with respect to the concentrations of the matrix solutions. Figure 3 shows the results obtained with $CsNO_3$, KNO_3, $Mg(NO_3)_2$, $Ni(NO_3)_2$, and $Ca(NO_3)_2$ as the matrices. The reason why we did not show the results of $NaNO_3$, $Ba(NO_3)_2$, and $Sr(NO_3)_2$ here is that their effects are similar to that of $Mg(NO_3)_2$.

It is seen that Mg does not exhibit a pronounced influence on the signal, Ba, Sr, and Na as well (not shown). K, Cs, and Ni can enhance Li DFWM signal intensity. For Cs, signal intensity increases rapidly to 1.32 times higher with increasing Cs concentration and then gets saturated with further increasing Cs concentration. Similarly, DFWM signal intensity increases with K concentration increasing to 1.3 times higher and then ends up with the saturation. As for Ni, signal intensity increases slowly to 1.15 times higher and then gets saturated. Comparatively, Ca demonstrates suppressing effect on DFWM signal intensity, and

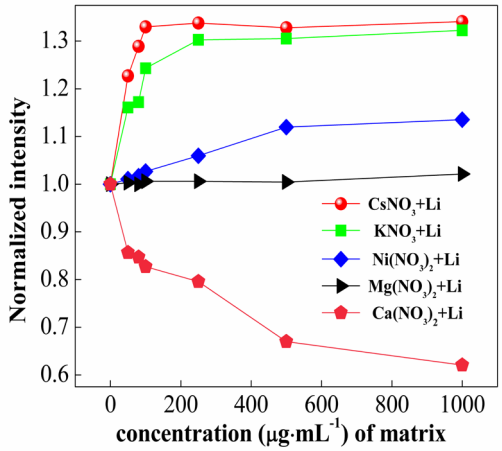

Fig. 3. Normalized Li (300 ng·mL^{-1}) DFWM signal intensity containing various major metallic elements at different concentrations.

DFWM signal intensity decreases with the concentration of increasing Ca.

With low ionization potential (5.4 eV), Li atoms are easily ionized at high temperature in the graphite furnace. The ionization process can be represented as

$$\mathrm{Li(g)}\leftrightarrow\mathrm{Li^{+}(g)+e.}$$

Due to ionization, the population of free Li atoms is reduced and Li DFWM signal intensity decreases accordingly. The ionization potentials of K (4.34 eV) and Cs (3.88 eV) are lower than Li, so K and Cs are more easy to ionize and lose electrons. The lost free electrons from K and Cs can be captured by Li^{+} to form free Li atoms. Abundant electrons can also effectively constrain the ionization of Li atoms. And therefore Li DFWM intensity is enhanced by K and Cs matrix. Since Cs has a lower ionization potential than K, Cs has a greater enhancement on the Li DFWM signal intensity.

During atomization process, a small part of analyte will vaporize in the form of gaseous molecules together with rapidly expanding matrix gases, which reduce the content of free Li atoms and cause the Li DFWM signal depression. Ni can stabilize numerous elements, for example, Sb, Se, As, and Bi[25,26]. The presence of Ni in Li solution may increase the stability of Li. Stabilization is ascribed to the formation of a more thermo stable compound or alloy between Li and Ni. Then the compound dissociates into free Li atoms completely at the atomization stage. In short, Ni prevents the loss of analyte at the ashing stage and Li DFWM intensity is enhanced accordingly.

In the case of Ca matrix, there are two types of interference mechanisms possible to account for the strong loss of Li free atoms[19,24]. Firstly, some Li are tightly wrapped in Ca matrix microcrystals, which prevent Li_2CO_3 from thermal dissociation during atomization process. The wrapped Li are carried out of the graphite furnace without being atomized. Secondly, thermo stable compounds are formed between Li and Ca, whose dissociation in the gas phase is incomplete. Both of the abovementioned mechanisms reduce the population of free Li atoms. Thus, the DFWM signals of Li are suppressed by Ca matrix.

We obtain 300 ng·mL^{-1} Li by mixing Li_2CO_3 solutions containing 600 ng·mL^{-1} Li, respectively, with $MgCl_2$, $SrCl_2$, NaCl, and $BaCl_2$ containing 10 μg·mL^{-1} Cl^{-} of the same volume. Then the Li DFWM signals in these chlorides are measured in sequence. Similarly, the measured data are all normalized to the one obtained with pure Li_2CO_3 solution containing 300 ng·mL^{-1} Li. The results are shown in Table 2. It is seen that DFWM signal of Li is suppressed to different extents by $MgCl_2$, $SrCl_2$, NaCl, and $BaCl_2$ matrices. The strongest suppression effect is observed by $MgCl_2$, followed by $SrCl_2$, NaCl, and $BaCl_2$. From the above investigation, Mg, Sr, Na, and Ba have no effects on Li DFWM signal. Therefore, we attribute these suppressing phenomena to the effect of Cl^{-}.

In the chloride matrix, the loss of Li is mainly originated from the gas phase reaction between the analyte atoms and matrix decomposition products. Cl is released when chloride is heated. It can be captured by free Li atoms to form LiCl molecule at the atomization stage. Due to the high bond-dissociation energy of LiCl (464 kJ·mol^{-1}), it hardly dissociate into free Li atoms and then vaporize out of the graphite furnace. The total number of Li atoms is reduced, thus Li DFWM signal is suppressed. The suppression effect depends on the concentration of Cl. The more Cl is released, the stronger the suppression effect is. From Table 2, we can see that although the content of Cl is the same among the four matrices, their effects on Li DFWM signal are different. This accounts for the R–Cl bond-dissociation energy. As shown in Table 2, Mg–Cl bond-dissociation energy is lowest, so $MgCl_2$ is easy to dissociate and much Cl is released. Comparatively, due to the high Ba–Cl bond-dissociation energy, $BaCl_2$ is difficult to dissociate and small amount of Cl is released. More Cl is released means more LiCl molecules are generated, and more Li atoms are lost. That is why Li DFWM signal is suppressed most by $MgCl_2$, whereas $BaCl_2$ almost has less effect on Li DFWM signal.

The above research indicates Li are always lost in the form of LiCl in the chloride samples. In order to get rid

Table 2. Normalized Li (300 ng·mL^{-1}) DFWM Signal Intensity Containing 5 μg·mL^{-1} Cl^{-} from Different Chlorides

Chlorides	$MgCl_2$	$SrCl_2$	NaCl	$BaCl_2$
R–Cl Bond-Dissociation Energy(kJ·mol^{-1})[24]	310	402	410	444
Normalized Intensity[a]	0.43603	0.67559	0.73782	0.86631

[a]Data represent the measured Li DFWM signal intensity normalized to the one obtained with pure Li_2CO_3 sample solution.

of such loss of Li, it is better to add a kind of matrix to form more stable chloride. It has been known that the compounds of B can react with chlorine to form stable chloride BCl_3 (B–Cl bond-dissociation energy 536 kJ·mol^{-1})[24]. Simultaneously, BCl_3 molecule can escape out of graphite furnace and eliminate Cl^- in the sample. Hence, Li atoms can keep inside of the graphite furnace. In the experiment, we take H_3BO_3 as modifier to eliminate the influence of chloride on Li analysis in NaCl samples by DFWM technique.

About 300 ng·mL^{-1} Li solutions are obtained by mixing 900 ng·mL^{-1} Li_2CO_3 solution containing 900 ng·mL^{-1} Li with various concentrations of NaCl (up to 900 μg·mL^{-1}) in the presence and absence of 30% H_3BO_3 in the same volume. Then we measure the signals with these mixtures in sequence and the signals normalized to the one measured with pure Li_2CO_3 solution containing 300 ng·mL^{-1} Li. The results are collected and plotted with respect to the concentration of NaCl (Fig. 4).

It is seen that Cl^- suppresses DFWM signal intensity and the intensity decreases with the concentration of increasing NaCl. Conversely, the signal remains constant when we mix H_3BO_3 into the mixtures solutions, which is due to the fact that H_3BO_3 can help NaCl matrix convert to a more stable form as BCl_3 instead of LiCl. During the atomization process, H_3BO_3 firstly decomposes into B_2O_3 and then gets converted to BCl_3 with chlorine under higher temperature. BCl_3 molecule can escape out of graphite furnace and eliminate the influence of chloride on Li analysis in NaCl samples.

In conclusion, we analyze Li element in Li_2CO_3 atomized in a graphite furnace using the DFWM method. The effects of acid anions, major metallic elements, and chlorides on Li DFWM signal intensity are studied. It is found that NO_3^-, Mg, Ba, Sr, and Na have no effects on Li DFWM signal. K, Cs, and Ni enhance the Li DFWM signal, whereas SO_4^{2-}, PO_4^{3-}, Cl^-, and Ca cause serious depression. Finally, we use H_3BO_3 to eliminate the interference of chloride. This work is of significance in trace Li analysis of actual samples with DFWM. The investigation provides valuable information in enhancing DFWM signal and reducing the detection limit. Simultaneously, it is also found that H_3BO_3 can also be taken as an efficient modifier to analyze other elements in chloride samples using DFWM.

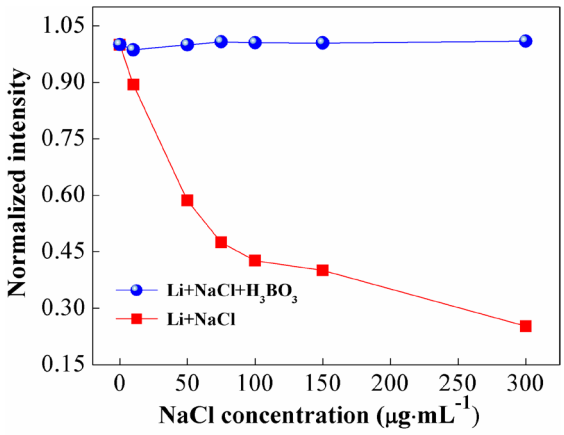

Fig. 4. Normalized DFWM signals of Li (300 ng·mL^{-1}) influenced by NaCl matrix with or without H_3BO_3.

This work was supported by the National "973" Plan Preliminary Study Special of China (Nos. 2012CB723407 and 2010CB434811), the Northwest University Science Foundation (No. 13NW12), and the Shaanxi Provincial Department of Education Project (No. 12JK0599).

References

1. S. C. Penniston-Dorland, G. E. Bebout, P. A. E. P. Strandmann, T. Elliott, and S. S. Sorensen, Geochim. Cosmochim. Acta **77,** 530 (2012).
2. X. Li, D. Qu, W. Wang, X. Zhao, L. Zhang, and X. Meng, Chin. Opt. Lett. **10,** 122101 (2012).
3. H. D. Wizemann, Spectrochim. Acta, Part B **63,** 539 (2008).
4. M. J. Marques, A. Salvador, A. E. Morales-Rubio, and M. de la Guardia, Microchem. J. **65,** 177 (2000).
5. X. Kong, Chin. Opt. Lett. **6,** 060417 (2008).
6. L. Kékedy-Nagy and E. A. Cordos, Talanta **52,** 645 (2000).
7. K. Weed and W. Tong, Appl. Spectros. **57,** 1455 (2003).
8. Z. W. Sun, Z. S. Li, B. Li, M. Aldén, and P. Ewart, Appl. Phys. B **98,** 593 (2010).
9. Y. P. Zhang, Z. G. Wang, Z. Q. Nie, C. B. Li, H. X. Chen, K. Q. Lu, and M. Xiao, Phys. Rev. Lett. **106,** 093904 (2011).
10. S. Huo, Z. Zhang, Z. Wu, H. Zheng, T. Liu, X. Xue, J. Song, and Y. Zhang, Chin. Opt. Lett. **9,** 121902 (2011).
11. K. K. Höinghaus, Progr. Energy Combust. Sci. **20,** 203 (1994).
12. R. L. Farrow and D. J. Rakestraw, Science **257,** 1894 (1992).
13. F. K. Mickadeit, S. Berniolles, H. R. Kemp, and W. G. Tong, Anal. Chem. **76,** 1788 (2004).
14. P. Ewart and S. V. O'Leary, Opt. Lett. **11,** 279 (1986).
15. X. Cheng, Z. Ren, J. Wang, Y. Miao, X. Xu, L. Jia, H. Fan, and J. Bai, Spectrochim. Acta, Part B **70,** 39 (2012).
16. F. M. Pereira, D. M. Brum, F. G. Lepri, and R. J. Cassella, Microchem. J. **117,** 172 (2014).
17. W. Zhang, R. Liu, W. Zhang, J. Zheng, and K. Xu, Chin. Opt. Lett. **10,** 083002 (2012).
18. G. A. Trapp, Anal. Biochem. **148,** 127 (1985).
19. S. Akman and H. I. Tekgul, Spectrochim. Acta, Part B **54,** 505 (1999).
20. B. Welz and M. Sperling, *Atomic Absorption Spectrometry* (Wiley-VCH, 1999).
21. S. Akman, B. Welz, and N. Tokman, Spectrochim. Acta, Part B **60,** 1349 (2005).
22. N. N. Meeravali, M. A. Reddy, and S. J. Kumar, Spectrochim. Acta, Part B **62,** 504 (2007).
23. Z. Wang, Y. Fu, Y. Song, G. Dai, F. Wen, J. Zhao, and Y. Zhang, Chin. Opt. Lett. **9,** 072701 (2011).
24. H. Sun, *Atomic Spectrum Analysis* (Higher Education Press, 2002).
25. N. Z. Ming and S. X. Quan, Spectrochim. Acta, Part B **42,** 937 (1987).
26. E. Bulska and K. Pyrzynska, Spectrochim. Acta, Part B **52,** 1283 (1997).